Organic & Biomolecular Chemistry

ROYAL SOCIETY OF CHEMISTRY

PAPER

View Article Online
View Journal

Cite this: DOI: 10.1039/d6ob00679e

Substituent effects on photoresponsive nitric oxide release by *N*-nitrosoaniline derivatives

Haruka Tsuchiya,[a] Osuke Yoshikawa,[b] Mei Harada,[a] Mikako Ogawa,[a,c] Yuhei Ohta,[b] Hidehiko Nakagawa[b] and Naoya Ieda*[a]

Received 28th April 2026,
Accepted 19th May 2026

DOI: 10.1039/d6ob00679e

rsc.li/obc

Nitric oxide (NO) is a short-lived signaling molecule mediating physiological functions such as vasorelaxation, and photocontrollable NO releasers that enable precise spatiotemporal control of NO release are useful tools for studying NO bioactivity as well as potential therapeutic agents for cardiovascular diseases. We recently developed NORD-2 as a photoinduced electron transfer (PeT)-triggered NO^+ releaser that responds to red light (λ 660 nm) by releasing NO in the presence of physiological concentrations of ascorbic acid or NO^+ in the absence of ascorbic acid. Here, we aimed to explore the structure–activity relationship by investigating the photoreactivity of derivatives having various substituents in the NO-releasing moiety. Replacement of NORD-2's methoxy group with all substituents examined reduced both NO^+ and NO release. In particular, the introduction of a dimethylamino group completely suppressed the photoreaction. Quantum chemical calculations revealed that the differences in photoreactivity originate from differences in the propensity for transition to the charge transfer (CT) excited state. Furthermore, when the energy of the CT excited state is low, deactivation to the ground state is likely to occur, which may prevent N–N bond cleavage. Our results identify suitable structures to promote efficient bond cleavage following PeT, which should be helpful for developing various photofunctional molecules.

Introduction

Controlling the bioactivities of molecules using light, as exemplified by caged compounds, offers unparalleled advantages in enabling precise spatiotemporal regulation.[1,2] Thus, elucidating the structure–activity relationships—specifically, understanding which structural features promote or suppress photoreactions—is critically important for the rational design of functional photoresponsive molecules.[3,4] Nitric oxide (NO) releasers are of particular interest because NO is a key signaling molecule with roles in vasodilation, immune function and the central nervous system,[5–7] but under physiological conditions, it has a short half-life of only a few seconds.[8] Therefore, NO-releasing small molecules are required for biological research and the clinical treatment of hypertension and angina pectoris.[9,10] In particular, photocontrollable NO releasers allow precise control of NO release and are important tools for studying NO bioactivity, as well as potential therapeutic agents for cardiovascular diseases.[6,7] We have developed photoinduced electron transfer (PeT)-type NO releasers that efficiently release NO in response to visible light.[11–13] PeT-type NO releasers consist of an antenna moiety, which absorbs light, and *N*-nitrosoaniline as an NO-releasing moiety. We previously reported NORD-2 (Fig. 1a, **1**) as a red light-responsive NO releaser with a high quantum yield for NO release (Φ_{NO}) and showed that it enabled photoregulation of the tension of rat aorta *ex vivo*.[14] More recently, photoactivation and photoredox activation of *N*-nitrosoaniline derivatives have attracted increasing attention as useful strategies for light-controlled NO release and related photochemical transformations.[15,16] However, NORD-2 releases NO only in the presence of a physiological concentration of ascorbic acid, whereas it releases NO^+ in the absence of ascorbic acid. The mechanism involved is as follows: when **1** is excited by light, PeT from the NO-releasing moiety to the antenna moiety occurs, generating a radical cation. In the absence of ascorbic acid, this intermediate directly releases NO^+ through mesolytic N–N bond cleavage. In contrast, in the presence of ascorbic acid, the radical cation intermediate is reduced by ascorbic acid and one-electron transfer from the dye generates the oxyhydrazine radical. This radical is very unstable, and the N–N bond is readily cleaved to release NO (Fig. 1b).[14] We hypothesized that changing the substituent of the NO releasing moiety would affect Φ_{NO}. To test this idea and identify key structural factors influencing the photoreaction, we synthesized a series of NORD-2 derivatives

[a]*Graduate School of Pharmaceutical Sciences, Hokkaido University, N12 W6, Kita-ku, Sapporo, Hokkaido, 060-0812, Japan. E-mail: ieda@pharm.hokudai.ac.jp*
[b]*Graduate School of Pharmaceutical Sciences, Nagoya City University, 3-1, Tanabe-dori, Mizuho-ku, Nagoya, Aichi, 467-8603, Japan*
[c]*WPI-ICReDD, Hokkaido University, N21 W10, Kita-ku, Sapporo, Hokkaido, 001-0021, Japan*

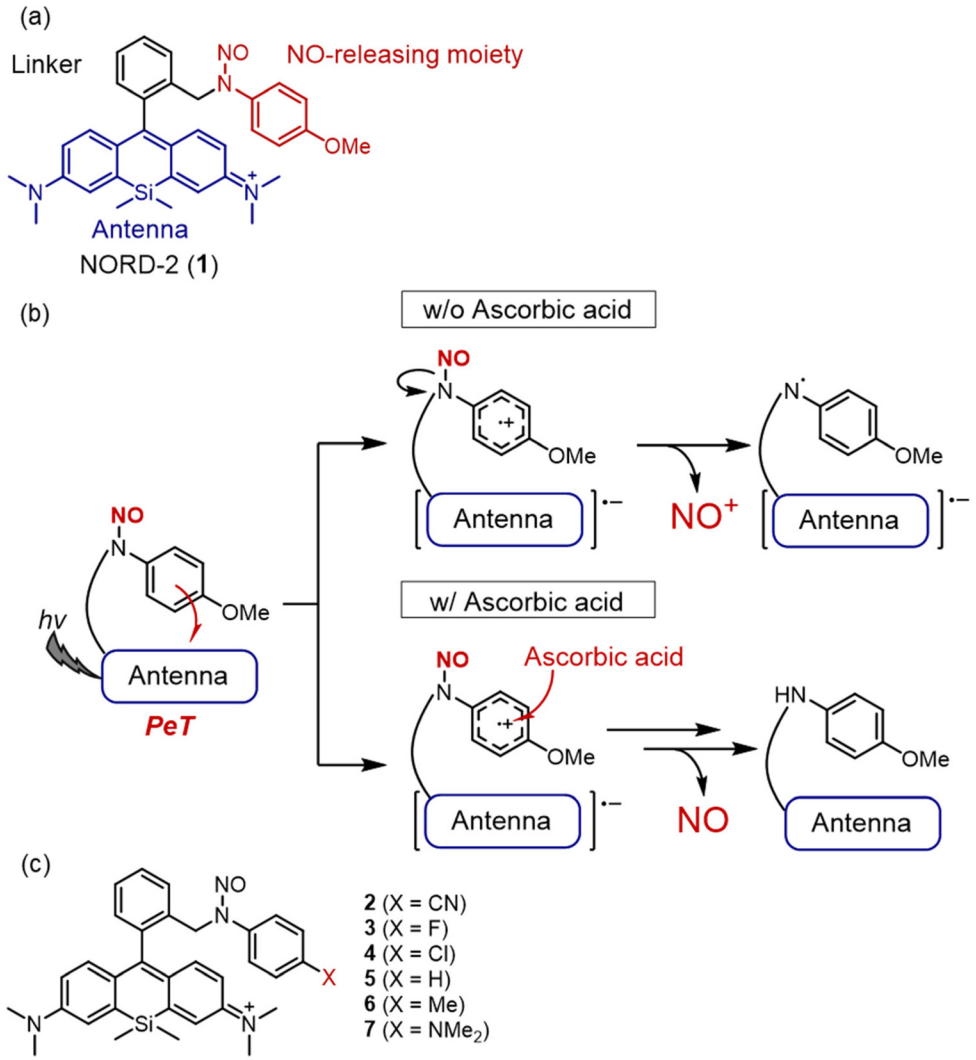

Fig. 1 (a) Structure of NORD-2 (**1**). (b) A plausible mechanism of photoinduced NO or NO^+ release from PeT-driven caged NOs. (c) NORD-2 derivatives substituted in the NO-releasing moiety.

with various substituents and evaluated their photoreactivity using a combination of experimental measurements and quantum chemical calculations.

Results and discussion

We designed a series of NORD-2 derivatives **2**–**7** bearing various electron-donating/withdrawing groups on the NO releasing moiety to investigate the substituent effect (Fig. 1c). Compounds **2**–**7** were synthesized according to Scheme 1. Briefly, the corresponding aniline derivatives were introduced into **8** by reductive amination, followed by nitrosation to obtain **2**–**7**.[11] In the case of **7**, intermediate **14** was readily oxidized and was therefore subjected to nitrosation without isolation. Compounds **2**–**7** were successfully synthesized and fully characterized.

Firstly, to evaluate the effect of the substituents on the photophysical properties, the absorption and fluorescence spectra of **2**–**7** were measured (Fig. 2a–f). These were all almost the same as those of **1**. Furthermore, compounds **1**–**6** exhibited nearly identical fluorescence quantum yields (Φ_F), though compound **1** showed a slightly lower value. In contrast, compound **7**, which bears a dimethylamino group, exhibited a markedly lower quantum yield, approximately one-fortieth of those of the other compounds. This difference is likely due to the strong electron-donating properties of the dimethylamino group, which would increase the electron density of the NO-releasing moiety, thereby promoting PeT, which competes with fluorescence emission.[17]

Next, to compare the photodecomposition rates, a solution of each compound (10 μM) in HEPES buffer was irradiated (LED, 660 nm, 9.9 mW cm^{-2}, 20 min). Decomposition rate constants (k) were calculated from the percentage decrease of the HPLC peak area (Fig. 3a) and compared with the Hammett

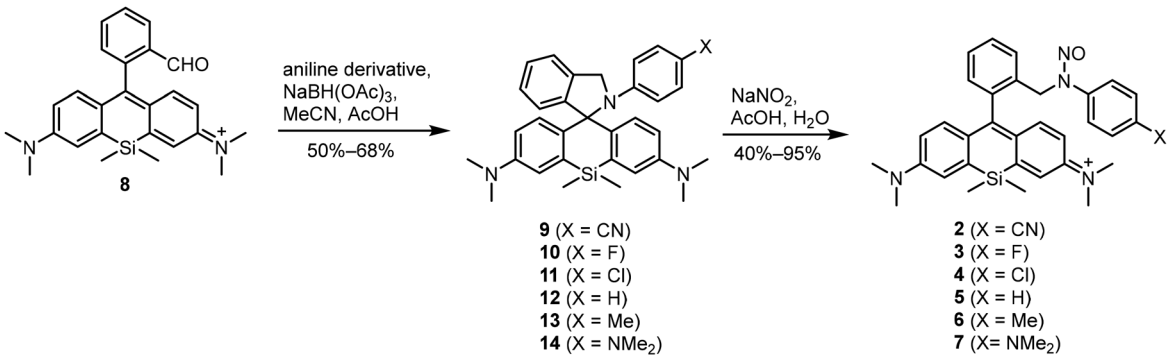

Scheme 1 Synthetic scheme to obtain **2**–**7**.

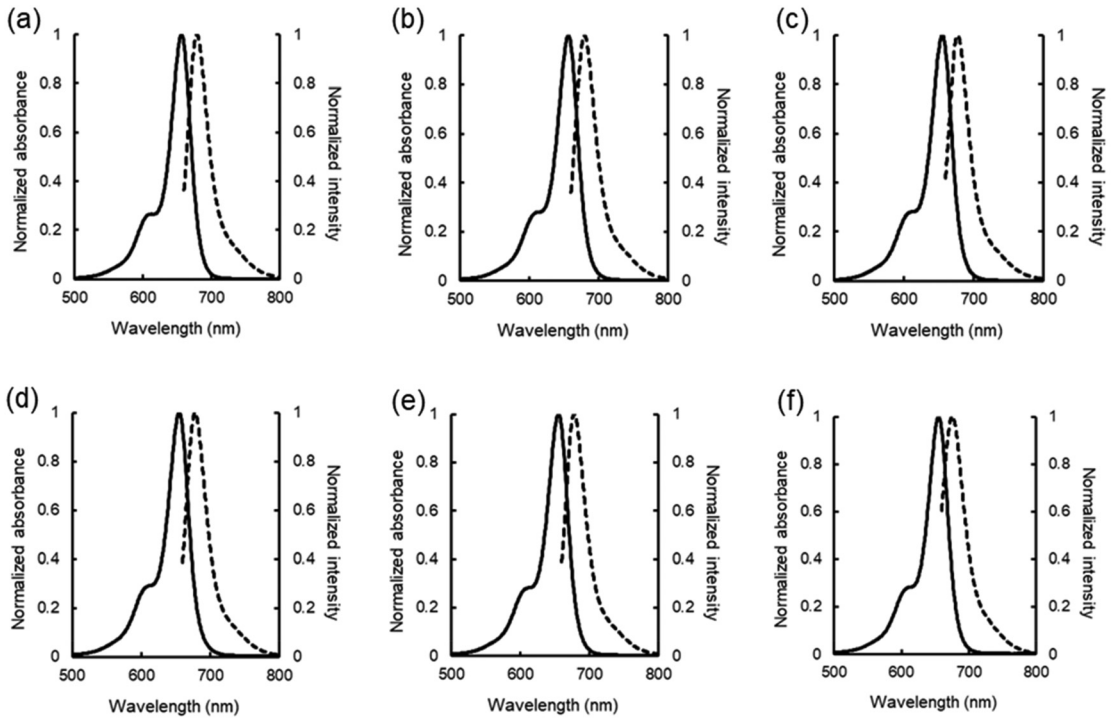

		1	2	3	4	5	6	7
Absorbance	λ_{max}	656	657	656	656	655	656	657
	$\varepsilon_{max} \times 10^{-5}$	1.5	1.0	1.2	1.1	1.0	1.2	0.64
Fluorescence	λ_{max}	676	679	679	680	677	678	675
	Φ_F	0.39	0.42	0.40	0.46	0.49	0.44	0.018

Fig. 2 Absorbance (solid line) and fluorescence (dashed line) spectra of a solution of **2** (a), **3** (b), **4** (c), **5** (d), **6** (e), or **7** (f). Each compound (10 μM) was dissolved in HEPES buffer (100 mM, pH 7.4, DMSO 0.1%). Maximum absorption wavelength (λ_{max} for absorbance), maximum extinction coefficient (ε_{max}), maximum fluorescence wavelength (λ_{max} for fluorescence), and fluorescence quantum yield (Φ_F) of each compound are shown in the table. The value of **1** is taken from ref. 14.

substituent constants, which roughly indicate the electron-withdrawing/donating character of the substituent (Fig. 3b).[18] The decomposition rate of **1** was the largest, while those of **2**–**7** showed no significant differences, suggesting that the decomposition rate is not strongly correlated with the electron-withdrawing/donating properties of the substituent on the NO-releasing moiety. Interestingly, compound **7**, which possesses a dimethylamino group and is thus considered highly favorable for PeT, underwent almost no photodecomposition.

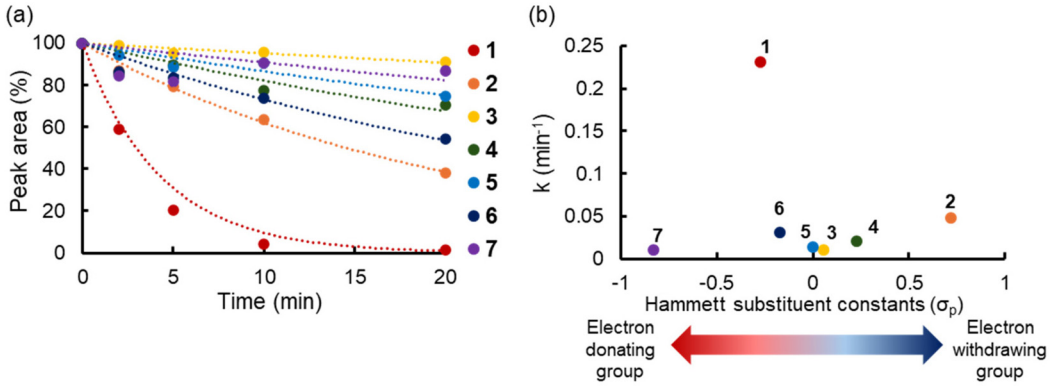

Fig. 3 (a) HPLC peak areas of solutions of **1–7** at each irradiation time. Each compound (10 μM) was dissolved in HEPES buffer (100 mM, pH 7.4, DMSO 0.1%). (b) Plot of the photodecomposition rate constant against the Hammett substituent constant (σ_p). σ_p of each substituent is taken from ref. 16.

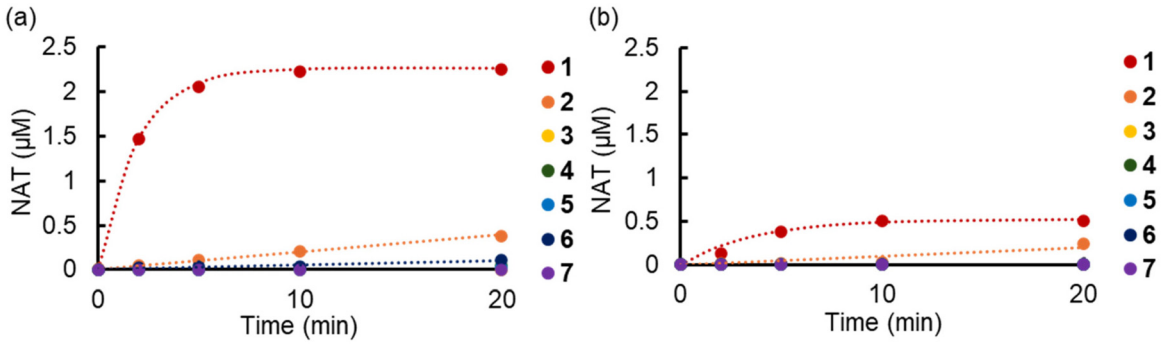

Fig. 4 (a) Amount of NAT produced in the absence of ascorbic acid. (b) Amount of NAT produced in the presence of ascorbic acid. Each compound (10 μM) and sodium ascorbate (10 μM) were dissolved in HEPES buffer (100 mM, pH 7.4, DMSO 0.1%).

To confirm that compounds **2–7** release NO^+ in response to photoirradiation and to investigate whether this release is suppressed (or converted to NO release) in the presence of ascorbic acid, 2,3-diaminonaphthalene (DAN) was utilized for NO^+ detection (Fig. 4). DAN is almost non-fluorescent and, although it does not readily react directly with NO, reacts with NO^+ to form 2,3-naphthotriazole (NAT), which shows strong fluorescence.[19] A solution of each synthesized compound (10 μM) and DAN (10 μM) in HEPES buffer was photoirradiated in the absence or presence of ascorbic acid (10 μM), and NAT formation was analyzed by HPLC. As shown in Fig. 4a, compound **1** exhibited the highest NO^+ release, whereas the release from the other compounds did not exceed 17% of that of **1**. In the presence of ascorbic acid, the NO^+ release from each compound was lower than that in its absence, suggesting that it was converted to NO release (Fig. 4b). Furthermore, decomposition rate constants did not change between the two conditions (Fig. 3a and S2a). These results confirm that **2–7** released NO^+ in the absence of ascorbic acid, whereas in its presence, a species other than NO^+ is generated *via* photodecomposition. According to the previous report, ascorbic acid is considered to reduce the charge-transfer (CT) state, rather than reacting directly with NO^+ or the excited state.[14] Therefore, the substituent effects in NORD-2 derivatives are unlikely to arise from the reduction by ascorbic acid.

We also investigated the photodecomposition products of **2–7** by means of LC-MS. It was previously shown that **1** forms spirocyclic compounds after releasing NO (Fig. S3a).[14] Indeed, LC-MS analysis revealed peaks corresponding to the mass-to-charge ratio (m/z) of the expected decomposition products for all compounds (Fig. S3b–h). As shown in our previous report, such closed-form/spirocyclic products are essentially nonfluorescent because disruption of the conjugated xanthene-like structure suppresses fluorescence.[14] In the chromatogram of **1**, additional peaks corresponding to aldehyde-type products were also detected, suggesting that part of the initially formed spirocyclic product underwent further oxidative transformation under the irradiation conditions.

The photoinduced release of NO from **1**, **2**, and **6**, which showed more than 40% degradation after 20 minutes of light irradiation (Fig. 3a), was investigated using an NO electrode (Fig. 5). Controlled irradiation in the absence of NO releasers did not increase the NO electrode signal, confirming that light irradiation itself did not interfere with NO detection (Fig. S4). Upon irradiation of HEPES buffer solutions of compounds **1**, **2**, and **6** with a 660 nm LED in the presence of ascorbic acid,

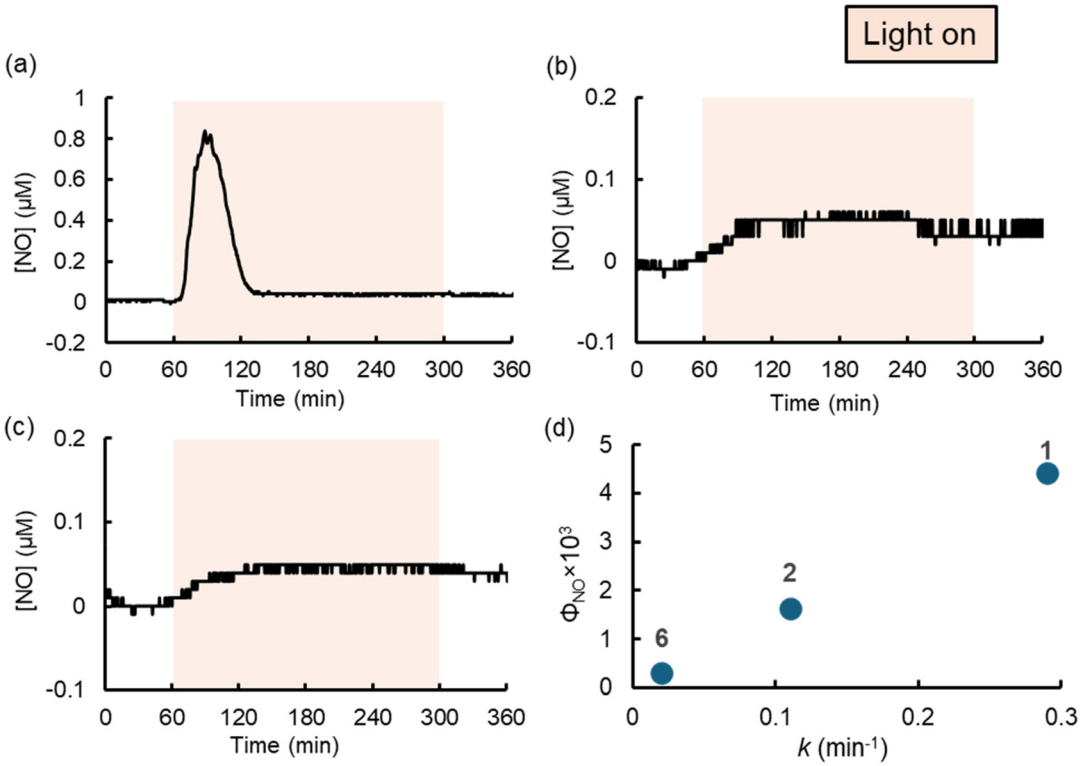

Fig. 5 (a)–(c) NO release detected using an NO electrode from a 10 μM solution (HEPES buffer 100 mM, pH 7.3, DMSO 0.1%) of **1** (a), **2** (b), and **6** (c). (d) Plot of the photodecomposition rate constant (horizontal axis) against Φ_{NO} (vertical axis) for **1**, **2**, and **6**.

light-dependent NO release was observed (Fig. 5a–c). The maximum NO concentration followed the order **1** > **2** > **6**, which is consistent with the order of the photodecomposition rates. Furthermore, the NO release quantum yield (Φ_{NO}) was measured to quantify the efficiency of NO release (Fig. 5d). A solution of each compound (10 μM) was irradiated at 660 nm with an Xe lamp in a fluorescence spectrophotometer (RF-5300PC, Shimadzu) and the NO concentration was recorded with an NO electrode. Using the Φ_{NO} of **1** as a reference, the Φ_{NO} values for **2** and **6** were calculated from the decomposition rates and absorbances. The Φ_{NO} value was correlated with the decomposition rate, as the faster-degrading compounds release NO more efficiently (Fig. 5d). The Φ_{NO} values also correspond well to the amount of NO^+ generated in the absence of ascorbic acid, indicating that the reduction of the intermediate resulted in NO release (Fig. S5). Thus, among compounds **1**, **2**, and **6**, the efficiency of NO release correlates well with the decomposition rate, which directly reflects the substituent effect.

We next conducted quantum chemical calculations to elucidate why **1** with a methoxy group is susceptible to photoreaction, whereas **7** with a dimethylamino group shows almost no photoreactivity despite its expected propensity for PeT. Since substituent effects on the reduction by ascorbic acid appeared unlikely, we first examined whether they contribute to the N–N bond cleavage. To this end, model radical anion intermediates **16**–**22** were employed, and the N–N bond lengths as well as the spin densities of the two nitrogen atoms (N1 and N2) were calculated (Fig. S6a). Spin density is an indicator of the localization of an unpaired electron, with larger absolute values corresponding to a higher probability of the electron residing on a given atom. The results are shown in Fig. S6b and c. In all model compounds, the N–N bond was significantly elongated, consistent with ease of bond cleavage, with no significant differences in the bond length. Similarly, no differences in spin density were found, and the larger spin density on N2 compared to N1 suggests a tendency to generate an NO radical. These results indicate that substituent effects have little impact on the N–N bond cleavage in the one-electron-reduced *N*-nitrosoaniline derivatives, and we inferred that the differences in reactivity originate from a differing propensity for PeT.

Next, to compare the likelihood of PeT occurrence, we calculated the energies of the π–π* excited state, CT excited state, and two distinct minimum energy conical intersections (MECIs): one lying between the π–π* state and the CT state (CT-MECI) and the other lying between the CT state and the ground state (GS-MECI). When **1**–**7** are excited by light, they transition to the π–π* excited state and subsequently transition to the CT excited state through PeT (Fig. 6a and b). As shown in Fig. 6c and S7, the energies of CT-MECI for **1** and **7** are lower than those for the other compounds and are almost the same as those of the π–π* excited state, probably because the strongly electron-donating groups promote transition to the

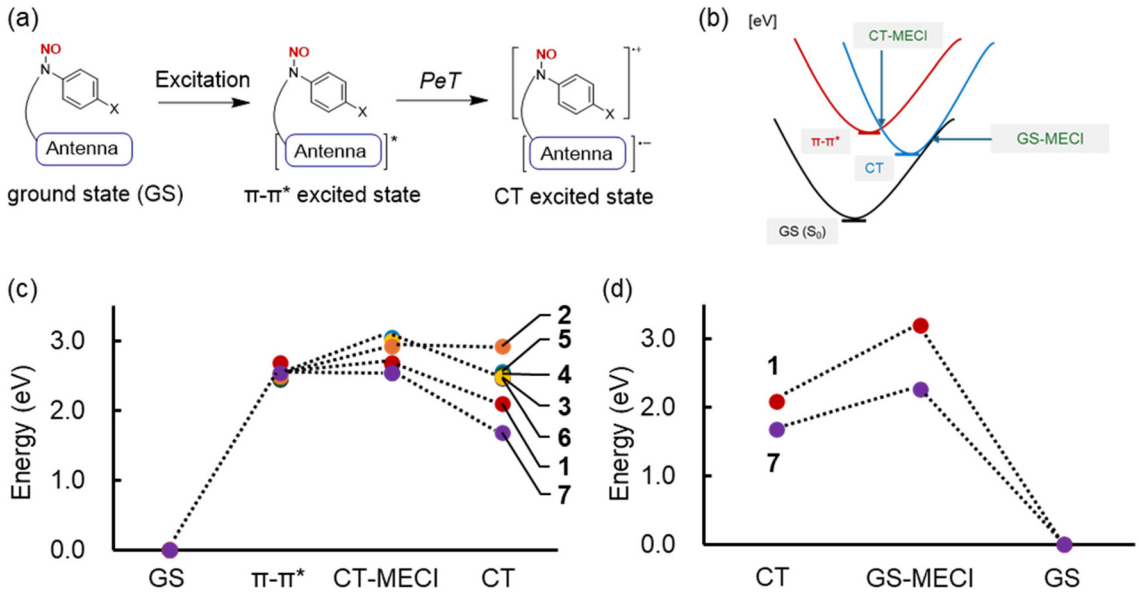

Fig. 6 (a) Excited states of NORD-2 derivatives. (b) Energy diagram of ground and excited states. (c) Energy of each excited state and CT-MECI of **1**–**7**. Calculation was conducted using ωB97XD/6-31G (d,p). (d) GS-MECI of **1** and **7**.

CT excited state. It should be noted that the calculated CT-MECI and CT excited-state energies provide only a qualitative guide to the accessibility of the CT excited state and do not necessarily quantitatively reflect the fluorescence quantum yields or photodecomposition rates. For example, although the calculated CT-MECI and CT excited-state energies of **3** are higher than those of **1**, the Φ_F value of **3** is comparable to that of **1**. The observed fluorescence is unlikely to originate predominantly from the CT excited state, because the emission spectra of **1**–**6** are nearly identical. Rather, the fluorescence is considered to arise mainly from the locally excited π–π* state, whereas the CT excited state is likely involved in subsequent non-emissive processes, including N–N bond cleavage and nonradiative deactivation. Therefore, the steady-state fluorescence quantum yield should not be interpreted as a direct measure of productive PeT efficiency. These results suggest that the substituent effects should be considered separately rather than interpreted by a simple one-parameter correlation with the CT excited-state energy. The comparison between **1** and **2** suggests that access to the CT excited state is one factor contributing to the high photoreactivity of **1**. Compound **2** exhibited higher CT-MECI and CT excited-state energies than **1**, indicating that transition to the CT state is less favorable in **2** (Fig. 6c and S7). This difference may partly account for the lower photodecomposition rate and Φ_{NO} of **2** compared with those of **1**. However, the comparison between **2** and **6** indicates that the CT excited-state energy alone does not determine the photoreactivity. Although the CT excited state of **6** is more stabilized than that of **2**, compound **2** showed a faster photodecomposition rate and a higher Φ_{NO}. This behavior may be related to the relaxation pathway after reaching the CT-MECI. In compound **2**, the CT-MECI and optimized CT excited state have nearly identical energies, suggesting that the system may reach the CT-state minimum without substantial additional structural relaxation after the π–π*/CT intersection (Fig. 6c and S7). This feature may contribute to the relatively efficient productive photodecomposition of **2** compared with **6**.

Although both **1** and **7** readily undergo transitions to the CT excited state, **1** decomposed in response to light with the highest efficiency among all compounds, whereas **7** showed the lowest reactivity. This behavior is probably attributed to the low energy of the CT excited state of **7**, which favors nonradiative deactivation to the ground state (GS) in accordance with the energy gap law.[20–22] This interpretation is further supported by the lower GS-MECI of **7** compared with that of **1** (Fig. 6d). The stabilized CT excited-state energy of **7** promotes PeT but would simultaneously facilitate deactivation to the ground state, thereby hindering NO release.

In conclusion, we synthesized NORD-2 derivatives with various substituents on the NO-releasing moiety and investigated their photoreactivity. Notably, compound **1** demonstrated the highest photoreactivity, while counterintuitively, **7** showed almost no photoreaction, in contrast to the conventional expectation that the dimethylamino group should strongly facilitate PeT. Quantum chemical calculations indicated that both methoxy and dimethylamino groups facilitate PeT owing to their strong electron-donating properties; however, the excessively stabilized CT excited state of **7** was suggested to promote relaxation from the CT excited state to the ground state, thereby suppressing photodecomposition (Fig. S8). Therefore, the highest Φ_{NO} observed for **1** may be attributed to an optimal electron density at the NO-releasing moiety, *i.e.*, high enough to promote PeT while not low enough to promote deactivation to the ground state. Thus, we suggest that consideration of the CT excited-state energy is important for accurate prediction of reactivity.

Methods

General methods

Proton and carbon nuclear magnetic spectra (^{1}H-NMR and ^{13}C-NMR) were recorded on a JEOL ECS-400 spectrometer using the indicated solvent. Chemical shifts (δ) are reported in parts per million relative to the internal standard, tetramethylsilane. Reagents used in the synthesis were purchased from Tokyo Chemical Industry, FUJIFILM Wako Pure Chemical, Merck, Kanto Chemical, and BLD Pharmatech unless otherwise noted. Thin layer chromatography (TLC) was performed using TLC silica gel 70 F254 glass plates (FUJIFILM Wako Pure Chemical). Medium pressure liquid chromatography (MPLC) was performed using Smart Flash Premium (Yamazen) and Universal Premium (Yamazen, silica gel) as the separation column and injection column, respectively.

General method for the preparation of 9–13

To a solution of **8** (1.0 equiv.) in MeCN/AcOH (10/1, 0.05 M) was added an aniline derivative (1.1 equiv. for **10–13** and 3.0 equiv. for **9**). $NaBH(OAc)_3$ (3.0 equiv.) was added, and the reaction mixture was stirred for 40 min. The reaction was quenched with 1 N NaOH aq. and the resulting mixture was extracted with CH_2Cl_2. The organic layer was dried over Na_2SO_4, filtered, and evaporated. The residue was purified by silica gel flash column chromatography (CH_2Cl_2/MeOH = 93/7 to 85/15 to 65/35) to obtain **9–13**.

Preparation of 9. 4-Aminobenzonitrile (14.0 mg, 0.11 mmol) was used as a substrate to obtain **9** according to the general method (26 mg, 0.051 mmol, 51%): ^{1}H-NMR (400 MHz, $CDCl_3$) δ 7.38 (d, J = 7.5 Hz, 1H), 7.23 (d, J = 8.6 Hz, 2H), 7.12 (ddd, J = 0.8, 7.4, 7.4 Hz, 1H), 7.03 (ddd, J = 0.4, 7.6, 7.6 Hz, 2H), 6.87 (d, J = 2.9 Hz, 2H), 6.77 (d, J = 9.0 Hz, 2H), 6.67 (d, J = 7.7 Hz, 1H), 6.54–6.49 (m, 4H), 5.18 (s, 2H), 2.91 (s, 12H), 0.67 (s, 3H) 0.60 (s, 3H); ^{13}C-NMR (100 MHz, $CDCl_3$) δ 150.90, 148.33, 147.30, 138.10, 132.90, 132.86, 131.45, 128.31, 126.54, 123.56, 122.73, 120.88, 115.85, 115.44, 113.96, 97.45, 77.30, 76.93, 56.19, 40.30; HRMS (ESI+) calcd, 515.25863; found, 515.26179 (−6.13 ppm).

Preparation of 10. 4-Fluoroaniline (12 mg, 0.11 mmol) was used as a substrate to obtain **10** according to the general method (35 mg, 0.068 mmol, 68%): ^{1}H-NMR (400 MHz, $CDCl_3$) δ 7.37 (d, J = 7.6 Hz, 1H), 7.09 (ddd, J = 1.1, 7.4, 7.4 Hz, 1H), 7.00 (ddd, J = 0.8, 7.5, 7.5 Hz, 1H), 6.89 (d, J = 2.9 Hz, 2H), 6.86 (d, J = 8.9 Hz, 2H), 6.73–6.68 (m, 3H), 6.55 (dd, J = 2.9, 9.0 Hz, 2H), 6.40 (dd, J = 4.4, 9.3 Hz, 2H), 5.15 (s, 2H), 2.91 (s, 12H), 0.69 (s, 3H) 0.59 (s, 3H); ^{13}C-NMR (100 MHz, $CDCl_3$) δ 155.97, 153.60, 151.59, 148.20, 140.65, 139.49, 132.95, 132.69, 128.63, 127.88, 126.18, 123.58, 122.71, 115.96, 115.53, 115.20, 114.98, 114.10, 114.03, 76.34, 60.49, 56.37, 40.40, 21.16, 14.32, 1.209; HRMS (ESI+) calcd, 508.25396; found, 508.25726 (−6.49 ppm).

Preparation of 11. 4-Chroloaniline (14 mg, 0.11 mmol) was used as a substrate to obtain **11** according to the general method (28 mg, 0.053 mmol, 53%): ^{1}H-NMR (400 MHz, $CDCl_3$) δ 7.38 (d, J = 7.7 Hz, 1H), 7.10 (ddd, J = 1.0, 7.4, 7.4 Hz, 1H), 7.01 (ddd, J = 0.8, 7.6, 7.6 Hz, 1H), 6.93 (d, J = 9.0 Hz, 2H), 6.89 (d, J = 3.0 Hz, 2H), 6.84 (d, J = 9.0 Hz, 2H), 6.69 (d, J = 7.8 Hz, 1H), 6.55 (dd, J = 3.0, 9.0 Hz, 2H), 6.42 (d, J = 9.0 Hz, 2H) 5.15 (s, 2H), 2.91 (s, 12H), 0.69 (s, 3H) 0.60 (s, 3H); ^{13}C-NMR (100 MHz, $CDCl_3$) δ 151.43, 148.24, 142.76, 139.16, 132.93, 132.43, 128.57, 128.45, 127.97, 126.27, 123.58, 122.72, 120.54, 115.93, 115.53, 114.85, 76.40, 56.20, 53.53, 40.39, 1.19; HRMS (ESI+) calcd, 524.22441; found, 524.22808 (−7.00 ppm).

Preparation of 12. Aniline (10 mg, 0.11 mmol) was used as a substrate to obtain **12** according to the general method (28 mg, 0.053 mmol, 53%): ^{1}H-NMR (400 MHz, $CDCl_3$) δ 7.36 (d, J = 7.5 Hz, 1H), 7.07 (ddd, J = 1.0, 7.4, 7.4 Hz, 1H), 6.98 (ddd, J = 1.9, 7.7, 7.7 Hz, 3H), 6.89–6.87 (m, 4H), 6.69 (d, J = 7.6 Hz, 1H), 6.54–6.47 (m, 5H), 5.17 (s, 2H), 2.89 (s, 12H), 0.68 (s, 3H), 0.59 (s, 3H); ^{13}C-NMR (100 MHz, $CDCl_3$) δ 151.59, 148.15, 144.13, 139.78, 132.79, 132.70, 128.64, 128.56, 127.84, 126.12, 123.60, 122.70, 115.98, 115.65, 115.51, 113.97, 76.29, 56.08, 40.43, 31.70, 22.77, 14.24, 1.17; HRMS (ESI+) calcd, 490.26338; found, 490.26687 (−7.12 ppm).

Preparation of 13. *p*-Toluidine (12 mg, 0.11 mmol) was used as a substrate to obtain **13** according to the general method (34 mg, 0.067 mmol, 67%): ^{1}H-NMR (400 MHz, $CDCl_3$) δ 7.36 (d, J = 7.4 Hz, 1H), 7.07 (ddd, J = 0.8, 7.4, 7.4 Hz, 1H), 6.98 (ddd, J = 0.5, 7.4, 7.4 Hz, 1H), 6.90–6.87 (m, 4H), 6.81 (d, J = 8.4 Hz, 2H), 6.69 (d, J = 7.7 Hz, 1H), 6.53 (dd, J = 2.9, 9.0, 9.0 Hz, 2H), 5.16 (s, 2H), 2.88 (s, 12H), 2.09 (s, 3H), 0.69 (s, 3H) 0.59 (s, 3H); ^{13}C-NMR (100 MHz, $CDCl_3$) δ 151.68, 148.12, 141.89, 139.99, 132.79, 129.21, 128.66, 127.78, 126.07, 126.07, 124.18, 123.59, 122.69, 115.98, 115.69, 113.79, 76.17, 56.12, 40.45, 20.32, 1.18; HRMS (ESI+) calcd, 504.27903; found, 504.28214 (−6.17 ppm).

General method for the preparation of 2–7

To a solution of **9–14** (1.0 equiv.) in AcOH (33 mM) was added a solution of $NaNO_2$ (1.1 equiv.) in water on an ice-water bath. The mixture was stirred for 20 min, quenched with 0.2 M HCl and extracted with CH_2Cl_2. The organic layer was dried over Na_2SO_4 and then evaporated. Purification of the residue by silica gel flash chromatography (CH_2Cl_2/MeOH = 93/7 to 85/15 to 65/35) gave **2–7** as a dark blue solid.

Preparation of 2. Compound **9** (71 mg, 0.14 mmol) was used as a substrate to obtain **2** according to the general method (32 mg, 0.055 mmol, 40%): ^{1}H-NMR (400 MHz, $CDCl_3$) δ 7.59 (d, J = 2.8 Hz, 2H), 7.54–7.44 (m, 3H), 7.36 (d, J = 8.9 Hz, 2H), 7.31 (d, J = 2.8 Hz, 2H), 7.11 (d, J = 7.6 Hz, 1H), 6.80 (d, J = 9.8 Hz, 2H), 6.64 (dd, J = 2.8, 9.6 Hz, 2H), 5.04 (s, 2H), 3.35 (s, 12H), 0.64 (s, 3H), 0.52 (s, 3H); ^{13}C-NMR (100 MHz, CD_3OD) δ 168.67, 156.88, 150.65, 146.89, 143.13, 140.39, 135.63, 135.01, 132.54, 131.98, 131.71, 130.24, 129.47, 123.52, 121.47, 116.30, 112.35, 51.05, 45.54, 42.20, 0.41; HRMS (ESI+) calcd, 544.25271; found, 544.25199 (+1.32 ppm).

Preparation of 3. Compound **10** (35 mg, 0.069 mmol) was used as a substrate to obtain **3** according to the general method (27 mg, 0.047 mmol, 69%): ^{1}H-NMR (400 MHz, $CDCl_3$) δ 7.51–7.41 (m, 2H), 7.35 (dd, J = 0.8, 7.8 Hz, 1H), 7.32 (d, J = 2.8 Hz, 2H), 7.23–7.18 (m, 2H), 7.12 (dd, J = 1.4, 7.3 Hz, 1H), 7.01 (ddd, J = 2.2, 7.6, 7.6 Hz, 2H), 6.85 (d, J = 9.6 Hz, 2H), 6.67

(dd, J = 2.8, 9.8 Hz, 2H), 4.99 (s, 2H), 3.34 (s, 12H), 0.64 (s, 3H), 0.54 (s, 3H); ^{13}C-NMR (100 MHz, CD_3OD) δ 168.98, 156.87, 150.67, 143.22, 140.53, 139.73, 135.29, 132.27, 131.68, 131.53, 130.01, 129.60, 124.45, 124.37, 123.46, 118.32, 118.09, 116.30, 46.53, 42.12, 0.26; HRMS (ESI+) calcd, 537.24804; found, 537.24769 (+6.51 ppm).

Preparation of 4. Compound **11** (35 mg, 0.069 mmol) was used as a substrate to obtain **4** according to the general method (27 mg, 0.047 mmol, 69%): ^{1}H-NMR (400 MHz, $CDCl_3$) δ 7.51–7.41 (m, 2H), 7.35 (dd, J = 0.8, 7.8 Hz, 1H), 7.32 (d, J = 2.8 Hz, 2H), 7.23–7.18 (m, 2H), 7.12 (dd, J = 1.4, 7.3 Hz, 1H), 7.01 (ddd, J = 2.2, 7.6, 7.6 Hz, 2H), 6.85 (d, J = 9.6 Hz, 2H), 6.67 (dd, J = 2.8, 9.8 Hz, 2H), 4.99 (s, 2H), 3.34 (s, 12H), 0.64 (s, 3H), 0.54 (s, 3H); ^{13}C-NMR (100 MHz, CD_3OD) δ 169.01, 156.95, 150.74, 143.31, 142.18, 140.55, 135.47, 135.03, 132.45, 132.09, 131.68, 131.57, 130.16, 129.67, 123.51, 123.43, 116.37, 46.31, 42.25, 0.44; HRMS (ESI+) calcd, 553.21849; found, 553.21804 (+8.13 ppm).

Preparation of 5. Compound **12** (25 mg, 0.050 mmol) was used as a substrate to obtain **5** according to the general method (27 mg, 0.047 mmol, 69%): ^{1}H-NMR (400 MHz, $CDCl_3$) δ 7.48–7.40 (m, 2H), 7.32 (d, J = 2.8 Hz, 2H), 7.30–7.19 (m, 6H), 7.11 (dd, J = 1.6, 7.3 Hz, 1H), 6.88 (d, J = 9.7 Hz, 2H), 6.66 (dd, J = 2.9, 9.6 Hz, 2H), 6.85 (d, J = 9.6 Hz, 2H), 6.67 (dd, J = 2.8, 9.8 Hz, 2H), 4.99 (s, 2H), 3.34 (s, 12H), 0.64 (s, 3H), 0.54 (s, 3H); ^{13}C-NMR (100 MHz, CD_3OD) δ 156.88, 150.68, 143.42, 143.22, 135.25, 132.21, 131.51, 131.44, 131.23, 129.88, 129.59, 129.57, 123.46, 123.43, 121.96, 121.94, 116.29, 113.40, 46.31, 42.10, 1.31, 0.22; HRMS (ESI+) calcd, 519.25746; found, 519.25616 (+2.50 ppm).

Preparation of 6. Compound **13** (32 mg, 0.063 mmol) was used as a substrate to obtain **6** according to the general method (33 mg, 0.058 mmol, 92%): ^{1}H-NMR (400 MHz, $CDCl_3$) δ 7.50–7.41 (m, 2H), 7.32 (dd, J = 2.9, 4.4 Hz, 3H), 7.13–7.10 (m, 1H), 7.08 (d, J = 4.5 Hz, 4H), 6.89 (dd, J = 4.6, 9.7 Hz, 2H), 6.71–6.66 (m, 2H), 4.97 (s, 2H), 3.35 (s, 12H), 3.00 (s, 3H), 0.63 (s, 3H), 0.54 (s, 3H); ^{13}C-NMR (100 MHz, CD_3OD) δ 157.07, 150.91, 143.52, 132.67, 132.41, 132.15, 132.14, 132.05, 132.02, 131.60, 131.56, 131.49, 130.04, 129.83, 123.59, 123.45, 122.25, 116.48, 42.29, 42.20, 0.42, 0.15; HRMS (ESI+) calcd, 533.27311; found, 533.27275 (+6.75 ppm).

Preparation of 7. To a solution of **8** (90 mg, 0.20 mmol) in anhydrous MeCN (2.6 mL) were added *N*,*N*-dimethyl-*p*-phenylenediamine (30 mg, 0.22 mmol) and AcOH (0.4 mL) followed by $NaBH(OAc)_3$ (127 mg, 0.60 mmol). The mixture was stirred at room temperature for 15 min, then the reaction was quenched with 1 M NaOH and the resulting mixture was extracted with CH_2Cl_2. The organic layer was dried over Na_2SO_4. After filtration and evaporation, the residue was dissolved in AcOH (2 mL). To this solution was added 0.11 M $NaNO_2$ (aq.) (2 mL) at 0 °C, and the mixture was stirred for 15 min. The reaction was quenched with 1 M HCl, and the resulting mixture was extracted with CH_2Cl_2. The organic layer was dried over Na_2SO_4. Filtration and evaporation followed by purification of the residue by silica gel flash chromatography (CH_2Cl_2/MeOH = 90/10 to 85/15 to 65/35) gave **7** as a dark blue solid (23 mg, 0.039 mmol, 19%): ^{1}H-NMR (400 MHz, $CDCl_3$) δ 7.49–7.40 (m, 2H), 7.33–7.30 (m, 3H), 7.09 (dd, J = 1.3, 7.5 Hz, 1H), 6.97 (dd, J = 2.1, 7.0 Hz, 2H), 6.84 (d, J = 9.5 Hz, 2H), 6.63 (dd, J = 2.9, 9.6 Hz, 2H), 6.56 (d, J = 9.2 Hz, 2H), 4.95 (s, 2H), 3.33 (s, 12H), 2.91 (s, 6H), 0.63 (s, 3H), 0.55 (s, 3H); ^{13}C-NMR (100 MHz, CD_3OD) δ 193.76, 169.21, 156.74, 152.69, 150.44, 143.26, 140.47, 135.77, 132.50, 132.04, 131.51, 131.36, 129.68, 124.17, 123.26, 116.16, 114.43, 47.06, 41.97, 41.69, 26.57, 0.035; HRMS (ESI+) calcd, 562.29966; found, 562.29886 (+1.42 ppm).

Measurements of absorption and fluorescence spectra. Absorption spectra of a solution of each compound (10 μM) in HEPES buffer (100 mM, pH 7.3, 0.1% DMSO) were recorded on an Agilent 8453 spectroscopy system (Santa Clara, CA, USA). Fluorescence spectra of a solution of each compound (10 μM) in HEPES buffer (100 mM, pH 7.3, 0.1% DMSO) or phosphate buffer (100 mM, indicated pH, 0.1% DMSO) were recorded on a fluorescence spectrometer (RF5300-PC; Shimadzu, Kyoto, Japan). The Φ_F values were calculated with reference to the Φ_F of the previously reported compound.[13]

Monitoring of photodecomposition by HPLC

A solution (total volume 10 mL) of each test compound (10 μM) in HEPES buffer (100 mM, pH 7.3, DMSO 0.1%) was irradiated using a device (CL-1501, Asahi Spectra) with a 660 nm LED head unit (CL-H1-660-9-1). The light intensity was 9.9 mW cm^{-2}. An aliquot of each solution (20 μL) was loaded onto a Shim-pack Velox C18 (150 mm × 4.6 mm) column fitted on a Shimadzu HPLC system, and the eluates were monitored with a UV detector (650 nm). MilliQ water containing 0.1% TFA (A) and MeCN containing 0.1% TFA (B) were used as developing solvents; 5% B (1.33 min) → 20% B (2 min) → 80% B (11.33 min) → 100% B (12 min) → 5% B (16 min).

Monitoring the formation of NAT using HPLC

A solution (total volume 10 mL) of each compound (10 μM) and 2,3-diaminonaphthalene (10 μM) in HEPES buffer (100 mM, pH 7.3, DMSO 0.1%) was irradiated with a 660 nm LED head unit (CL-H1-660-9-1). The light intensity at 660 nm was 9.9 mW cm^{-2}. An aliquot of each solution (20 μL) was loaded onto a Shim-pack Velox C18 (150 mm × 4.6 mm) column fitted on a Shimadzu HPLC system, and the eluates were monitored with a fluorescence detector (ex. 360 nm, em. 460 nm) and a UV detector (650 nm). MilliQ water containing 0.1% TFA (A) and MeCN containing 0.1% TFA (B) were used as developing solvents: 0 min, B 5% → 2 min, B 5% → 3 min, B 20% → 15 min, B 80% → 17 min, B 80% → 18 min, B 100% → 23 min, 100% → 24 min, B 5% → 30 min, B 5%. This experiment was also conducted in the presence of sodium ascorbate (10 μM) using the same procedure.

Identification of decomposition products

A solution (total volume 10 mL) of each compound (10 μM) in HEPES buffer (100 mM, pH 7.3, DMSO 0.1%) was irradiated using a 660 nm LED head-unit (CL-H1-660-9-1). The light intensity at 660 nm was 9.9 mW cm^{-2}. An aliquot of each solu-

tion before and after irradiation (20 μL) was loaded onto an ODS3 (150 mm × 2.1 mm) column fitted on a Shimadzu LC-MS system, and the eluates were monitored with a UV detector (650 nm). MilliQ water containing 0.1% TFA (A) and MeCN containing 0.1% TFA (B) were used as developing solvents: 0 min, B 5% → 2 min, B 5% → 3 min, B 20% → 15 min, B 80% → 17 min, B 80% → 18 min, B 100% → 23 min, 100% → 24 min, B 5% → 30 min, B 5%.

Calculation of quantum yield of NO release (Φ_{NO})

A solution of each compound (10 μM) in 100 mM HEPES buffer (pH 7.3, total volume: 3 mL) containing 0.1% DMSO was placed in a plastic cuvette and irradiated at 660 nm (bandwidth: 10 nm) for 1 min with the Xe lamp of a fluorescence spectrometer, RF5300 (Shimadzu). The amount of NO released was measured with an ISO-NOP (World Precision Instruments) and recorded on a LabChart7 (ADInstruments). The Φ_{NO} values were calculated with reference to the Φ_{NO} of the previously reported compound **1** (3.85×10^{-3}).[13]

Quantum chemical calculations

All calculations were carried out with the Gaussian16 program.[23] The optimization of minimum energy conical intersection (MECI) was performed using GRRM23.[24] The molecular structure optimizations were conducted by means of density functional theory (DFT) and time-dependent DFT (TD-DFT) calculations with the ωB97X-D and UωB97X-D[25] functionals using the 6-31G (d,p) basis set.[26,27] In this study, the Gibbs free energy was adopted as the basis for discussion. All stationary structures have no imaginary frequency.

Author contributions

Conceptualization, N. I. and H. N.; methodology, N. I. and H. N.; investigation, H. T., O. Y., M. H. and Y. O.; formal analysis, H. T., O. Y., M. H., Y. O. and N. I.; data curation, H. T., O. Y., M. H., Y. O. and N. I.; writing – original draft preparation, H. T.; writing – review and editing, M. H., M. O., H. N. and N. I.; visualization, H. T. and Y. O.; supervision, M. O., Y. O., H. N. and N. I.; project administration, M. O., H. N. and N. I.; and funding acquisition, M. O., H. N. and N. I. All authors have read and agreed to publish this manuscript.

Conflicts of interest

There are no conflicts to declare.

Data availability

The data supporting this article have been included as part of the supplementary information (SI). Supplementary information is available. See DOI: https://doi.org/10.1039/d6ob00679e.

Acknowledgements

We gratefully acknowledge the assistance of the Instrumental Analysis Division, Global Facility Center, Creative Research Institution, Hokkaido University, for ESI-MS exactive mass spectrometer assistance and their insight and expertise that greatly contributed to this study. This work was supported in part by JSPS KAKENHI grant numbers JP 25K09865 (N. I.), JP23H02612 (H. N.), the Daiichi Sankyo Foundation of Life Science (N. I.), the Mochida Memorial Foundation for Medical and Pharmaceutical Research (N. I.), the JSPS Program for Forming Japan's Peak Research Universities (J-PEAKS, JPJ00420230001) at Hokkaido University, and the Photo-excitonix Project at Hokkaido University. We thank Yuka Okura for assistance with the NO electrode control experiment.

References

1 P. Klán, T. Šolomek, C. G. Bochet, A. Blanc, R. Givens, M. Rubina, V. Popik, A. Kostikov and J. Wirz, *Chem. Rev.*, 2013, **113**, 119–191.
2 R. Weinstain, T. Slanina, D. Kand and P. Klán, *Chem. Rev.*, 2020, **120**, 13135–13272.
3 N. Ieda, A. Nakamura, N. Tomita, K. Ohkubo, R. Izumi, Y. Hotta, M. Kawaguchi, K. Kimura and H. Nakagawa, *RSC Adv.*, 2023, **13**, 26375–26379.
4 N. Ieda, M. Tachi, M. Noda, M. Harada, Y. Hotta, K. Kondo, H. Tsuchiya, M. Ogawa, M. Kawaguchi and H. Nakagawa, *RSC Adv.*, 2026, **16**, 11964–11971.
5 L. J. Ignarro, G. M. Buga, K. S. Wood and G. Chaudhuri, *Proc. Natl. Acad. Sci. U. S. A.*, 1987, **84**, 9265–9269.
6 C. Bogdan, *Nat. Immunol.*, 2001, **2**, 907–916.
7 R. A. Hopper and J. Garthwaite, *J. Neurosci.*, 2006, **26**, 11513–11521.
8 T. Nagano and T. Yoshimura, *Chem. Rev.*, 2002, **102**, 1235–1269.
9 C. Napoli and L. J. Ignarro, *Annu. Rev. Pharmacol. Toxicol.*, 2003, **43**, 97–123.
10 E. Nishio and Y. Watanabe, *Eur. J. Pharmacol.*, 1997, **339**, 245–251.
11 N. Ieda, Y. Hotta, N. Miyata, K. Kimura and H. Nakagawa, *J. Am. Chem. Soc.*, 2014, **136**, 7085–7091.
12 H. Okuno, N. Ieda, Y. Hotta, M. Kawaguchi, K. Kimura and H. Nakagawa, *Org. Biomol. Chem.*, 2017, **15**, 2791–2796.
13 N. Ieda, Y. Hotta, A. Yamauchi, A. Nishikawa, T. Sasamori, D. Saitoh, M. Kawaguchi, K. Kimura and H. Nakagawa, *ACS Chem. Biol.*, 2020, **15**, 2958–2965.
14 N. Ieda, Y. Yoshikawa, N. Tomita, K. Ohkubo, Y. Hotta, M. Kawaguchi, K. Kimuraa and H. Nakagawa, *Chem. Commun.*, 2022, **58**, 8420–8423.
15 T. J. Martins, C. Parisi, J. G. Pinto, I. P. R. Brambilla, M. Malanga, J. F. Strixino and S. Sortino, *ACS Med. Chem. Lett.*, 2024, **15**, 857–863.
16 Y. Chai, L. Shangguan, H. Yu, Y. Sun, X. Huang, Y. Zhu, H. Wang and Y. Liu, *Adv. Sci.*, 2024, **11**, 2198–3844.

17 T. Kowada, J. Kikuta, A. Kubo, M. Ishii, H. Maeda, S. Mizukami and K. Kikuchi, *J. Am. Chem. Soc.*, 2011, **133**, 17772–17776.
18 C. Hansch, A. Leo and R. W. Taft, *Chem. Rev.*, 1991, **91**, 165–195.
19 P. Damiani and G. Burini, *Talanta*, 1986, **33**, 649.
20 M. Bixon, J. Jortner, J. Cortes, H. Heitele and M. E. Michel-Beyerle, *J. Phys. Chem.*, 1991, **98**, 7289–7299.
21 Y. Wang, J. Ren and Z. Shuai, *Nat. Commun.*, 2023, **14**, 5056.
22 S. Jiang, Y. He, J. H. Brandt, L. Zhao and J. Chen, *J. Phys. Chem. Lett.*, 2023, **14**, 10482–10488.
23 M. J. Frisch, G. W. Trucks, H. B. Schlegel, G. E. Scuseria, M. A. Robb, J. R. Cheeseman, G. Scalmani, V. Barone, G. A. Petersson, H. Nakatsuji, X. Li, M. Caricato, A. V. Marenich, J. Bloino, B. G. Janesko, R. Gomperts, B. Mennucci, H. P. Hratchian, J. V. Ortiz, A. F. Izmaylov, J. L. Sonnenberg, D. Williams-Young, F. Ding, F. Lipparini, F. Egidi, J. Goings, B. Peng, A. Petrone, T. Henderson, D. Ranasinghe, V. G. Zakrzewski, J. Gao, N. Rega, G. Zheng, W. Liang, M. Hada, M. Ehara, K. Toyota, R. Fukuda, J. Hasegawa, M. Ishida, T. Nakajima, Y. Honda, O. Kitao, H. Nakai, T. Vreven, K. Throssell, J. A. Montgomery Jr., J. E. Peralta, F. Ogliaro, M. J. Bearpark, J. J. Heyd, E. N. Brothers, K. N. Kudin, V. N. Staroverov, T. A. Keith, R. Kobayashi, J. Normand, K. Raghavachari, A. P. Rendell, J. C. Burant, S. S. Iyengar, J. Tomasi, M. Cossi, J. M. Millam, M. Klene, C. Adamo, R. Cammi, J. W. Ochterski, R. L. Martin, K. Morokuma, O. Farkas, J. B. Foresman and D. J. Fox, *Gaussian 16, Revision C.01*, Gaussian, Inc., Wallingford CT, 2016.
24 S. Maeda, Y. Harabuchi, Y. Sumiya, M. Takagi, K. Suzuki, M. Hatanaka, Y. Osada, T. Taketsugu, K. Morokuma and K. Ohno, GRRM23 see https://iqce.jp/GRRM/index_e.shtml (accessed date Jan 8, 2026).
25 J.-D. Chai and M. Head-Gordon, *Phys. Chem. Chem. Phys.*, 2008, **10**, 6615–6620.
26 W. J. Hehre, R. Ditchfield and J. A. Pople, *J. Chem. Phys.*, 1972, **56**, 2257–2261.
27 P. C. Hariharan and J. A. Pople, *Theor. Chim. Acta*, 1973, **28**, 213–222.